ELSEVIER

Experimental Hematology

Experimental Hematology 2008;■:■–■

Differentiating human multipotent mesenchymal stromal cells regulate microRNAs: Prediction of microRNA regulation by PDGF during osteogenesis

Loyal A. Goff[a], Shayne Boucher[b], Christopher L. Ricupero[a], Sara Fenstermacher[a], Mavis Swerdel[a], Lucas Chase[b], Christopher Adams[b], Jonathan Chesnut[b], Uma Lakshmipathy[b], and Ronald P. Hart[a]

[a]*W. M. Keck Center for Collaborative Neuroscience and Rutgers Stem Cell Research Center, Rutgers University, Piscataway, NJ., USA;* [b]*Stem Cells and Regenerative Medicine, Invitrogen Corporation, Carlsbad, Calif., USA*

(Received 21 February 2008; revised 8 May 2008; accepted 12 May 2008)

Objective. **Human multipotent mesenchymal stromal cells (MSC) have the potential to differentiate into multiple cell types, although little is known about factors that control their fate. Differentiation-specific microRNAs may play a key role in stem cell self-renewal and differentiation. We propose that specific intracellular signaling pathways modulate gene expression during differentiation by regulating microRNA expression.**

Materials and Methods. **Illumina mRNA and NCode microRNA expression analyses were performed on MSC and their differentiated progeny. A combination of bioinformatic prediction and pathway inhibition was used to identify microRNAs associated with platelet-derived growth factor (PDGF) signaling.**

Results. **The pattern of microRNA expression in MSC is distinct from that in pluripotent stem cells, such as human embryonic stem cells. Specific populations of microRNAs are regulated in MSC during differentiation targeted toward specific cell types. Complementary mRNA expression analysis increases the pool of markers characteristic of MSC or differentiated progeny. To identify microRNA expression patterns affected by signaling pathways, we examined the PDGF pathway found to be regulated during osteogenesis by microarray studies. A set of microRNAs bioinformatically predicted to respond to PDGF signaling was experimentally confirmed by direct PDGF inhibition.**

Conclusion. **Our results demonstrate that a subset of microRNAs regulated during osteogenic differentiation of MSCs is responsive to perturbation of the PDGF pathway. This approach not only identifies characteristic classes of differentiation-specific mRNAs and microRNAs, but begins to link regulated molecules with specific cellular pathways.** **© 2008 ISEH - Society for Hematology and Stem Cells. Published by Elsevier Inc.**

Mesenchymal stem cells or multipotent mesenchymal stromal cells (MSC), though commonly isolated from adult bone marrow, have also been isolated from such diverse biological sources as bone [1], skeletal muscle, lung, deciduous teeth [2], and human umbilical cord [3], and are defined by their ability to attach to a solid surface when other cells present in crude preparations from these tissues do not [4]. Due to the lack of a single definitive marker, MSC are generally characterized by the presence and absence of a combination of surface antigens. It has been universally accepted that MSC lack the common hematopoietic markers such as CD45, CD34, and CD14 [5]. More recently, STRO-1, CD44, CD90, CD73, and CD105 have emerged as positive markers of MSC [5–8]. The self-renewal capacity of MSC, thought to be limited, is known to be enhanced under specific culture conditions, such as serum concentration, cell-seeding density, and inclusion of growth factors, such as fibroblast growth factor-2 [9–11]. These various culture methods may be a major source of the heterogeneous nature of the MSC cell population. Several studies have indicated the capability of MSC to

Offprint requests to: Uma Lakshmipathy, Ph.D., Stem Cells and Regenerative Medicine, Invitrogen Corporation, 5781 Van Allen Way, Carlsbad, CA 92008; E-mail: Uma.Lakshmipathy@invitrogen.com

0301-472X/08 $–see front matter.
doi: 10.1016/j.exphem.2008.05.004

differentiate into mesenchymal lineages, such as adipose tissue, bone, cartilage, tendon, muscle, and hematopoietic-supporting stroma [12–19]. The multilineage differentiation potential of clonally derived cells within a MSC population have been shown to be variable [5,20–25], further demonstrating the heterogeneous nature of the defined MSC population.

Nevertheless, the possibility of obtaining MSC from an autologous source and their ability to differentiate into a variety of connective tissue types makes them ideal candidates for cell therapy. The unquestioned therapeutic potential of MSC is reflected in current clinical usage for treating children with osteogenesis imperfecta, hematopoietic recovery, and for bone tissue regeneration [26–28].

Understanding key regulatory pathways and molecules involved in maintaining MSC in either their undifferentiated state or during the process of differentiation allows for a better handle on expanding and culturing these cells in large scale for therapeutic applications. Examination of gene expression profiles has revealed dynamics between MSC, progenitor cells, and committed differentiated cells [29,30]. Recently, the importance of epigenetic regulation via microRNA in controlling stem cell activities has been recognized [31–37]. Understanding these regulatory mechanisms may help to design novel processes for production of specific therapeutic cells for transplant.

MicroRNAs (miRNA), short (17 – 24 nucleotides), noncoding RNAs that have been identified in various organisms, including mammalian cells, are thought to play a key role in several biological processes [38–41]. It has been suggested that >30% of protein coding genes in humans are regulated by miRNA [42]. More recently, a unique set of miRNA have been shown to be associated with embryonic stem cells [43–48]. These miRNAs are expressed at high levels in several human embryonic stem cell (ESC) and human embryonal carcinoma cell (EC) lines [49,50] and decrease upon differentiation into embryoid body (EB) for 2 weeks in culture [50], supporting their association with the stem cell state. Furthermore, strategies to knock down miRNA levels in ESC cells demonstrate that miRNAs are essential for differentiation, likely by suppressing stem cell self-renewal programs [44,51]. The understanding of integrated gene expression and epigenetic miRNA mechanisms should be important for the characterization of stem cells and their progeny.

Studies of gene expression patterns are valuable not only for distinguishing cell types during differentiation, but also for revealing signature patterns reflecting the regulation of specific intracellular signaling pathways. Work in MSC by our collaborators recently analyzed standard microarray results to identify several such pathways active during MSC differentiation [52], including the platelet-derived growth factor (PDGF) pathway acting during osteogenesis. We sought to extend this work to predict the novel regulation of miRNA transcription as a mediator of, at least, translational repression during differentiation. Specifically, we hypothesized that ~~specific~~ groups of miRNAs would be regulated during MSC differentiation and that a subset of these groups could be associated with PDGF-responsive transcription factors. In order to test this hypothesis, we first assessed differentiation status of several MSC isolates by cell markers or gene expression. Because variability between MSC isolates is known to be a complicating factor, we also examined a pooled preparation of MSC. MSC and differentiation-specific miRNA expression patterns were determined and used to predict PDGF-responsive ~~pathways.~~ Finally, PDGF regulation of the predicted miRNAs was tested by inhibition of the PDGF pathway. These studies not only identify miRNAs indicative of MSC differentiation patterns, but also demonstrate that extracellular signals contribute to miRNA regulation during differentiation, supporting a role for miRNAs during MSC development.

Materials and methods

Cells

MSC from four independent donors were purchased from Cambrex (at passage 2) with the tissue acquisition numbers 1678C (18 years old, African American, male), 1822A (22 years old, African American, male), 1832A (18 years old, African American, male), and 1271C (23 years old, African American, female), and were designated as donors 1, 2, 3, and 4, respectively. A pooled MSC sample comprised of a mixture of these four donors' MSC that were mixed together in equal numbers and cryopreserved. Cells were diluted to 1 million cells per vial and frozen in MSC culture media plus 15% dimethyl sulfoxide (Sigma-Aldrich, St Louis, MO, USA) at a controlled rate to −70°C by using a cell freezer box. Cell stocks were transferred to liquid nitrogen storage after 24 hours. An additional MSC line (designated as donor 5) was obtained from Dr. Rick Cohen (Rutgers University, Newark, NJ, USA) and Dr. Eric Hume (Cooper University Hospital, Camden, NJ, USA). The donor was a 39-year-old male.

Culture

MSC were seeded at 3000 cells per cm^2 and expanded on tissue culture–treated plastic dishes (~~Corning Costar~~). MSC culture media was composed of Dulbecco's modified Eagle's medium/F12 (Invitrogen, Carlsbad, CA, USA), 10% fetal bovine serum, 1 × GlutaMAX (Invitrogen), modified Eagle's medium nonessential amino acids, 10 mM HEPES, and 0.5 μg/mL gentamycin (Invitrogen). Cells were fed on alternate days and passaged when 80% confluence was reached. Illumina gene expression and NCode miRNA analysis was carried out with samples that were grown less than a month in culture (P10 or lower).

Differentiation

MSC were expanded in culture and seeded in T125 flasks for differentiation into either adipocytes or osteocytes. A fraction of these cells were stored as day 0 samples. Cells were also seeded in parallel on chamber slides for differentiation. Samples were stained or harvested for RNA isolation at 7, 14, or 22 days of differentiation.

Adipocyte differentiation was initiated by seeding MSC at a density of 20,000 cells per cm^2 in the presence of adipogenic differentiation media composed of MSC growth media with 0.5 mM isobutyl-methylxanthine (Sigma-Aldrich), 10 μM bovine insulin (Sigma-Aldrich), 1 μM dexamethasone (Sigma-Aldrich), and 200 μM indomethacin (Sigma-Aldrich).

Osteoblast differentiation was initiated by seeding MSC at a density of 5000 cells per cm^2 in the presence of osteogenic differentiation media composed of MSC growth media with 10 mM glycerol-2-phosphate (Sigma-Aldrich), 50 μM L-ascorbic acid (Sigma-Aldrich), and 100 nM dexamethasone (Sigma-Aldrich).

Chondroblast differentiation was initiated by seeding MSC at a density of 8×10^5 cells per tube in a 15 mL conical tube in 0.5 mL chondrogenic differentiation media composed of MSC growth media with 10 ng/mL [illegible] forming growth factor-β1 (~~R&D Systems~~), 50 nM L-ascorbic acid (Sigma-Aldrich) and 6.25 μg/mL bovine insulin (Sigma-Aldrich).

Staining

MSC were stained using antibodies specific against the surface antigens CD45, CD34, CD44, CD73, and CD105. Samples were run on FACSAria (BD Biosciences, CA, USA) and data analyzed using FloJo (Tree Star Inc., OR, USA).

Differentiation samples set up in chamber slides were stained with either Oil Red O for adipocytes, ~~Von Kossa~~ staining for osteocytes or Alcian blue for chondrocytes. Cells in chamber slides were fixed with 100 μL freshly prepared 4% formaldehyde/Dul-'s phosphate-buffered saline (D-PBS) solution made from 37% formaldehyde stock solution for 30 minutes at room temperature. The formaldehyde solution was discarded and wells rinsed three times with D-PBS.

Adipocytes. After fixation, cells were rinsed with 70% ethanol and incubated with 0.3% freshly prepared Oil Red O (Sigma-Aldrich) working solution (three parts 0.5% Oil Red O with two parts deionized water, filtered through #42 Whatman paper) for 1 hour at room temperature. Cells were rinsed twice with 70% ethanol. Cells were rinsed twice with deionized water, counter stained with Dapi (Invitrogen, D3571) and visualized under light or fluorescence microscope.

Osteoblasts. ~~After fixation cells were rinsed three times with D-PBS and incubated with 5% silver nitrate for 10 minutes in the dark. Cells were rinsed three times with deionized water and exposed to bright light for 15 to 60 minutes. Cells were again rinsed three times with deionized water and visualized under light microscope.~~

Chondroblasts. After fixation, cells were rinsed twice with D-PBS and incubated with 1% Alcian Blue solution for 30 minutes at room temperature. Cells were then rinsed with 0.1% HCl solution to remove excess stain and visualized under light microscope.

AG-370 treatment

MSC (10,000 cells per cm^2) were seeded in six-well plates and allowed to recover for 72 hours. PDGF receptor kinase inhibitor AG-370 (Sigma-Aldrich, 2 μM) was added to cells. After 7 days, cells were harvested in TRIzol and RNA extracted for quantitative polymerase chain reaction (qPCR) analysis of miRNA.

mRNA expression analysis

Total cellular RNA was amplified and labeled for Illumina BeadArray analysis as reported earlier [53]. Labeled, amplified material (~700 ng per array) was hybridized to the Illumina Bead Chip according to manufacturer's instructions (Illumina, Inc., San Diego, CA, USA). Array data processing and analysis was performed using Illumina BeadStudio software, GeneSpring (Agilent) and BioConductor/R (http://www.bioconductor.org).

Enrichment of miRNA

MiRNA was isolated from Trizol-extracted total RNA using the PureLink miRNA Isolation Kit (Invitrogen) according to recommended protocol. The amount of miRNA was quantified using a spectrophotometer and its purity assessed by electrophoresis on a 15% ~~Nupage~~ urea-TBE gel (Invitrogen) and/or by running on a Bioanalyzer Nano RNA chip (Agilent).

MiRNA expression using NCode microarrays

For exploratory analysis of miRNA regulation in differentiating MSCs, samples (n = 1) of pooled-donor MSCs were differentiated for 7 or 14 days following the protocols for osteoblasts, adipocytes, or chondroblasts. Undifferentiated MSCs were included as a reference. The dual-color dye swap method [54] was used to study miRNA expression differences between undifferentiated and differentiated MSCs. Five-hundred nanograms of the enriched miRNA was labeled with the FlashTag (~~Genisphere, Inc.~~) direct labeling system and hybridized to NCode multispecies miRNA arrays [55] as described earlier [56] based on a loop design, balanced with respect to array, dye, and sample. By using a balanced design, sources of unwanted variation can be minimized [57]. Arrays were scanned, aligned, and median spot intensities were obtained using a GenePix 4000B scanner ~~(Molecular Devices, Inc.)~~. Data analysis methods are described in the Supplemental Methods.

PDGF pathway transcription factor–binding site predictions

To determine whether MSC-regulated miRNAs were enriched for the PDGF pathway, predicted promoter regions were obtained from miRNAs declared as significant and scanned for transcription factor (TF) binding sites from TFs predicted to be regulated by the PDGF pathway (Fig. 5A). A 5-kb region upstream of each miRNA gene was arbitrarily selected from human reference genome (hg18 assembly, NCBI Build 36.1) as an estimate for the transcriptional control region. Using pathway analysis software (Pathway Architect; Stratagene), mammalian cell surface receptors in the PDGF pathway were identified and a comprehensive literature search located all downstream transcription factors known to be regulated by this pathway. Seven transcription factors were identified (Fig. 5A). The 5-kb upstream region sequences were scanned with position weight matrices using ~~Transfac~~ Pro MATCH (version 11.2; Biobase) [58]. This process was repeated for 24 nonsignificant miRNAs with expression levels greater than background. These predictions were used as a representative set of "unregulated" miRNAs present in this system. The number of significant binding sites identified for this grouping of miRNAs is predicted to be characteristic of a random sample. Using a paired-sample *t*-test, the number of binding sites identified by ~~Transfac~~ MATCH was compared between significant and nonsignificant miRNAs. In order to predict specific miRNAs to be regulated by the PDGF

pathway, Z-tests were used to compare the number of significant binding sites for each ~~significant~~ miRNA with a mean number of binding sites across all regulated and nonregulated miRNA upstream regions.

qPCR

qPCR for adipogenic and osteogenic marker mRNAs was carried out using 20-ng cDNA templates prepared from DNase-treated total RNA isolated from MSC, differentiated adipocytes and osteocytes. The C_t value obtained for the gene of interest was normalized to a housekeeping gene, either β2 microglobulin or glyceraldehyde 3-phosphate dehydrogenase (GAPDH), as indicated, to obtain the ΔC_t values. $\Delta\Delta C_t$ values were then obtained by subtracting the ΔC_t values for each gene of interest against ΔC_t values for the control sample. Results expressed as fold change in expression relative to the control sample was calculated using the equation $RQ = 2^{-\Delta\Delta Ct}$.

NCode miRNA qPCR was performed and differences in miRNA expression between samples determined using the relative quantification method as described earlier [56]. Briefly, the C_t values of the samples were normalized to the C_t values of GAPDH, a housekeeping gene. Resulting values were further normalized to the corresponding undifferentiated MSC. Fold difference in gene expression of the sample from the reference undifferentiated cells was calculated using the equation $RQ = 2^{-\Delta\Delta Ct}$.

Results

Characterization of MSC

Because MSC are both variable by source and difficult to identify using simple markers, we began by testing cultures for several markers. Pooled cultures of four MSC donors (see Materials and Methods) were propagated on plastic dishes and the adherent cells further characterized for the absence and presence of surface antigens that are characteristic of MSC [59]. Fluorescein-activated cell sorting analysis of MSC demonstrates cells negative for the hematopoietic lineage markers CD45 and CD34 and positive for CD44, CD73, and CD105 (Fig. 1A). The identity of the cells as MSC was further confirmed based on their differentiation potential. The pooled MSC cells were differentiated at early passages into adipocytes, osteoblasts, and chondroblasts for 7 and 14 days. MSC from three independent donors with fewer than 10 passages were induced to differentiate into adipocytes or osteocytes for 22 days. Uniform differentiation of MSC into adipocytes, osteoblasts, and chondroblasts were determined based on Oil Red, ~~Von Kossa~~, and Alcian Blue staining, respectively (Fig. 1B). Based on these assays, we conclude that these cells, culture methods, and differentiation methods are appropriate.

To characterize cells in more detail using gene expression patterns, we conducted mRNA expression analysis on undifferentiated MSCs as well as cells differentiated using adipocytic or osteogenic protocols used in the study. A detailed description of the analysis of gene expression results can be found in the Supplemental Methods. For this analysis, we assayed individual donor cells at multiple passage numbers to identify genes that were consistently regulated. To focus on genes explaining differences between cell phenotypes (MSC, adipocytes, or osteocytes), expressed genes were tested for significant changes by cell type using the Welch's *F*-test with a 5% false discovery rate (FDR) [60], resulting in 1384 genes being selected (Supplemental Table 1). Selected genes were further partitioned using post-hoc analysis (Student-Newman-Keuls) into groups that distinguish cell types. One-hundred and sixty-seven genes differentiated MSC from osteocytes, and 94 genes distinguished MSC from adipocytes. Assembling these with the entire analysis of variance (ANOVA)–selected genes into a Venn diagram (Fig. 1C), we identify 48 genes shared between the two post-hoc groups. Forty-six genes uniquely distinguish adipocytes from MSC (including ACACB, CEBPA, FASN, LIPE, MVD, and PLIN—see Supplemental Table 1 for a complete list of significantly different mRNAs), while 119 genes uniquely distinguish osteocytes from MSC (including ADAM19, AOX1, AURKA, DPT, LEP, LEPR, MGP, PTHR1, and TIMP4). The 243 genes found on at least one of the post-hoc groups are marked in Supplemental Table 1 with asterisks marking membership within each of the post-hoc groups.

The raw signal intensities of known MSC, adipocyte, or osteoblast markers in all samples were examined further (Table 1). This list includes genes selected as part of the ANOVA list (marked with an asterisk) as well as those that were excluded from statistical analysis due to infrequent expression (denoted with a dagger). This Table also demonstrates the variability between individual donor cultures (see relative standard error of mean compared with the mean). This variability is another reason why some known differentiation markers were not selected by ANOVA. Of the markers associated with MSC that were clearly higher in expression level relative to adipocytes or osteocytes were Col21A1 (mean 65-fold lower in osteocytes, 18-fold lower in adipocytes) and PDGFRA (1.8-fold and 2.6-fold lower, respectively). Adipocyte differentiated cells from all three donors showed a clear up regulation of adipocytic markers relative to their undifferentiated cells or osteocyte differentiated cells, such as FABP4, LEP, LPL, and SREBF1. Among markers previously associated with osteocytes, POSTN and BGLAP were found to have expression patterns matching expectations. Gene expression patterns clearly indicate appropriate patterns of differentiation of these two cell types, validating the cells and differentiation protocols.

PDGF pathway analysis

In a parallel study, our collaborators performed a detailed analysis of predicted pathways regulated during MSC differentiation using microarrays [52]. Their work identified,

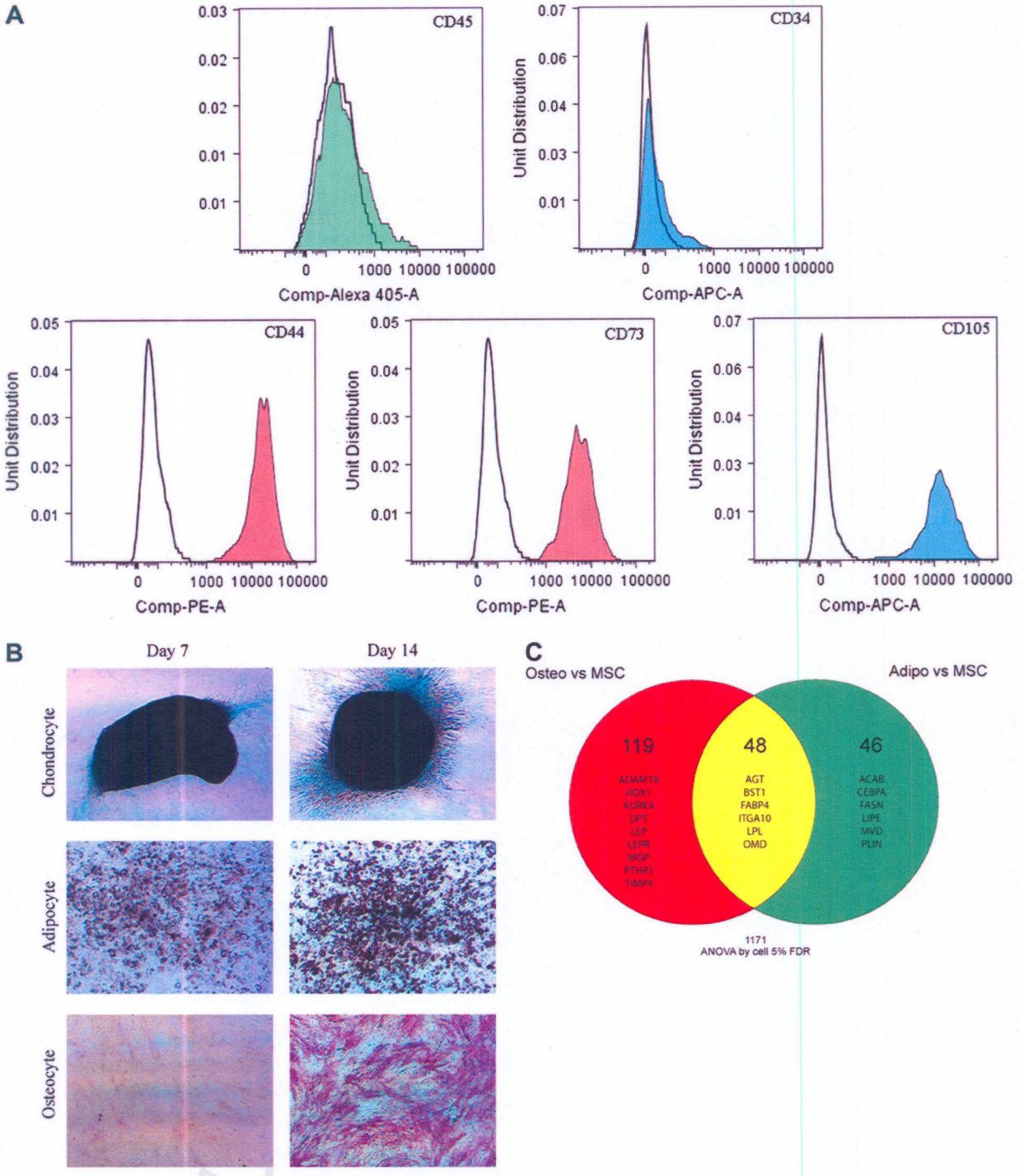

Figure 1. Characterization of mesenchymal stromal cells (MSC) and differentiation protocols A preparation of pooled MSC from four individual isolates (see Materials and Methods) was assessed for cellular markers before and after differentiation. (**A**) Fluorescein-activated cell sorting analysis for the absence (CD34, CD45) or presence (CD44, CD73, CD105) of surface antigens. Shaded peaks represent antibody labeled cells while the blank peaks are antibody isotype controls. (**B**) MSC cells differentiated into chondroblasts, adipocytes, osteoblasts for 7 and 14 days and subsequently stained with Alcian Blue, Oil Red, and ~~Von Kossa~~ staining, respectively. (**C**) Comparison of post-hoc subsets of mRNAs. Individual donors (donor 1 cultured at 7 or 8 passages and Donors 2 or 3 cultured at 10 passages) were assessed for gene expression by Illumina BeadChip arrays (see **Supplemental Methods**). A Venn diagram compares the overlap between 243 genes selected as differentially expressed between MSC and osteoblasts (red) or adipocytes (green) with the 48 overlapping genes labeled in yellow. Selected examples of genes in each category are shown. These results, along with known MSC markers shown in **Table 1** and the analysis of variance–selected genes in **Supplemental Table 1**, demonstrate that each cell isolate exhibits appropriate cellular markers and validates cell sources as well as differentiation protocols.

Table 1. Expression patterns of known mesenchymal stem cell differentiation markers

Specificity	Gene symbol	Illumina transcript ID	MSC	Adipo	Osteo	Description	UniGene ID	Entrez gene ID
Adipocyte	*FABP4	GI_4557578-S	400.5 ± 265.36	20,932.5 ± 4857.31	28.3 ± 10.67	Fatty acid binding protein 4, adipocyte	Hs.391561	2167
	*LPL	GI_4557726-S	95.4 ± 36.42	10,304.8 ± 2360.04	1.3 ± 2.57	Lipoprotein lipase	Hs.180878	4023
	*CEBPA	GI_28872793-S	119.5 ± 48.35	2818.9 ± 542.17	48.9 ± 7.27	CCAAT/enhancer binding protein (C/EBP), α	Hs.76171	1050
	PPARG	GI_20336230-A	470.7 ± 57.79	2788.1 ± 822.11	17.9 ± 10.35	Peroxisome proliferator-activated receptor gamma	Hs.162646	5468
	PGD	GI_40068517-S	198.0 ± 50.67	1933.7 ± 560.00	429.3 ± 56.51	Phosphogluconate dehydrogenase	Hs.464071	5226
	*LEP	GI_4557714-S	1746.5 ± 776.09	1477.7 ± 485.87	10.2 ± 1.74	Leptin	Hs.194236	3952
	*SREBF1	GI_22547194-S	553.8 ± 165.11	1004.1 ± 187.68	192.5 ± 9.39	Sterol regulatory element binding transcription factor 1	Hs.592123	6720
Osteocyte	POSTN	GI_5453833-S	1871.8 ± 740.57	101.0 ± 65.00	3206.4 ± 1091.90	Periostin, osteoblast specific factor	Hs.136348	10631
	BGLAP	GI_6005831-S	224.7 ± 19.29	158.0 ± 23.35	361.5 ± 45.60	Bone γ-carboxyglutamate (gla) protein (osteocalcin)	Hs.530479	11243
	†ALPI	GI_13787191-S	5.2 ± 8.86	28.8 ± 7.76	13.2 ± 7.50	Alkaline phosphatase, intestinal	Hs.37009	248
	†SPP1 (OPN)	GI_38146097-S	419.9 ± 318.25	12.8 ± 4.85	9.7 ± 1.24	Secreted phosphoprotein 1 (osteopontin)	Hs.313	6696
	†RUNX2	GI_10863884-S	-0.6 ± 0.54	–5.6 ± 1.28	-9.6 ± 1.99	Runt-related transcription factor 2	Hs.535845	860
MSC	VIM	GI_4507894-S	10,458.0 ± 2159.34	12,398.5 ± 1724.50	17,530.6 ± 3878.75	Vimentin	Hs.642813	7431
	*ANXA2	GI_4757755-S	8279.6 ± 1988.74	6004.0 ± 586.20	13,698.9 ± 2187.90	Annexin A2	Hs.511605	302
	PDGFRA	GI_15451787-S	2251.3 ± 434.88	877.1 ± 211.46	1251.5 ± 260.93	Platelet-derived growth factor receptor, α polypeptide	Hs.74615	5156
	THY1	GI_24475732-S	1875.8 ± 660.88	1072.8 ± 383.72	2431.3 ± 188.53	Thy-1 cell surface antigen; synonyms: CD90		
	ENG (CD105)	GI_4557554-S	736.9 ± 72.56	221.2 ± 92.75	1765.2 ± 227.50	Endoglin	Hs.76753	2022
	FZD2	GI_5922012-S	537.1 ± 9.04	261.5 ± 81.29	1202.5 ± 198.59	Frizzled homolog 2	Hs.142912	2535
	*CD44	GI_21361192-S	229.0 ± 32.87	220.1 ± 44.68	1098.6 ± 134.15	CD44	Hs.502328	960
	†COL21A1	GI_18780272-S	185.0 ± 68.76	11.5 ± 11.28	-0.3 ± 4.75	Collagen, type XXI, α1	Hs.47629	81578
	*BST1	GI_4757873-S	27.1 ± 8.65	–2.7 ± 5.42	343.1 ± 50.35	Bone marrow stromal cell antigen 1	Hs.169998	683
Housekeeping	B2 M	GI_37704380-S	11,351.1 ± 1472.97	8040.0 ± 889.31	11,908.4 ± 1482.55	β-2-microglobulin	Hs.534255	567

MSC = mesenchymal stem cell.

EXPHEM2340_proof ■ 28-6-2008 3-48-42

EQ1

among others, genes predicted to be regulated by the PDGF pathway were found to be regulated during adipocyte, chrondrocyte, and osteocyte differentiation. The requirement for this pathway was tested using AG-370, a Tyrphostin inhibitor of PDGF signaling, which produced fewer osteocytes and an absence of mineralized bone nodules [52], indirectly indicating the requirement for PDGF signaling during osteocyte differentiation. Of course, the PDGF pathway is not primarily known for its role in osteogenesis and is likely only one of many pathways required for differentiation [61]. However, the presence of several PDGF-pathway genes in our ANOVA list (e.g., PDGFRB, PDGFA, PDGFD, PDGFRL, NFKB1, and STAT3, Supplemental Table 1) lends additional support to the conclusion that PDGF mediates at least a portion of the osteogenesis program. Because mRNAs specific for PDGF signaling are expressed, because MSC have been found to express PDGF receptors (at least CD140B) [62], and because PDGF signaling has been found to be required for osteogenic differentiation [52], we predict that PDGF will regulate miRNAs as part of its mechanism.

Global miRNA expression

Before identifying potential targets of the PDGF pathway, we needed to identify overall patterns of miRNA regulation. An exploratory miRNA expression study was conducted on pooled MSC samples, as well as MSCs differentiated into each of three distinct cell types. Using NCode miRNA microarrays, samples of undifferentiated MSCs, adipo-, osteo-, and chondrogenic differentiated MSCs were assayed to determine expression levels for all known human miRNAs. We first examined which miRNA demonstrated significant regulation across any of the four conditions. Forty-four probes detecting 31 unique mature miRNAs ($p < 0.05$, FDR 5%) from the microarray ANOVA testing of hypothesis 1 (Supplemental Methods) were identified as differentially expressed between any of the cell types (Fig. 2A). Interestingly, most of the miRNAs highly expressed in human embryonic stem cells [50] were absent in MSC, while some markers associated with differentiating cells, such as miR-125, were expressed in MSC.

Pearson correlations were calculated to determine the relatedness between samples using global miRNA expression values. In this analysis, D7 and D14 adipocytes were highly correlated ($r = 0.99$), as well as D7 and D14 chondroblasts ($r = 0.91$). In addition, D14 osteoblasts were highly correlated with chondroblasts ($r = 0.90$), reflective of their shared cellular origin. Thus, samples with known biological relationships were found to be correlated based on miRNA expression patterns.

Some of the probes detected on the miRNA array were designed against nonhuman but similar miRNA sequences [55]. This was expected due to the similarity among paralogous miRNAs from different species as well as the inability to distinguish short RNAs having only a 1-nt or 2-nt difference [55]. Turning our attention to the 27 unique human mature miRNAs detected by these probes exclusively, a K-means cluster analysis was used to compare the expression patterns of significant miRNAs. This analysis groups miRNAs into clusters with similar levels of expression across the different samples (Fig. 2B). The data were fit to four clusters ($k = 4$), producing the best fit of merit compromise between number of clusters and residuals. Two miRNAs could not be consistently assigned to one of the four clusters, likely due to distributed membership in multiple clusters. Mean cluster expression patterns suggest the presence of miRNAs specific to each cellular type. As expected, miRNAs with previously defined, tissue-specific expression patterns were associated with their correct tissue types (e.g., miR-143 and miR-145 enrichment in adipocytes). Novel miRNA associations appear in this analysis as well (e.g., miR-638 and miR-663 expression exclusively in chondroblasts). This result identifies sets of miRNAs demonstrating significant regulation during the cell-type specific differentiation of MSCs, and suggests that differences across the resulting phenotypes can be associated with the differential expression of specific miRNAs.

The majority of the significantly regulated miRNAs appear to be selected primarily for their differences between the osteogenic samples and all other cell types (see clusters 1 and 2, Fig. 2B), suggesting that these miRNAs may be important for bone formation. This result drove us to test explicitly which miRNAs demonstrate significant differences between osteo-differentiated MSCs and all other cell types. The osteoblast-specific miRNAs agreed with those found in K-means clusters exhibiting increased expression in osteocytes. This confirms the identity of a subset of miRNAs that are expressed primarily in differentiating osteoblasts. Additionally, this analysis provides a target set for testing the effect of key regulatory pathways on the expression of putatively osteogenic miRNAs.

Validation of microarrays by miRNA qPCR

As validation of the NCode array data, qPCR was performed for a selection of the miRNAs from the significant list (Fig. 3; comparisons between undifferentiated cultures and osteo-differentiated cultures). We chose to assay osteogenic differentiation after only 7 days because the microarray results predicted that specific changes would be found this early in the process and because we wished to determine whether miRNA changes would precede, and possibly predict, differentiation choices. Triplicate cultures of MSC from either the pooled MSC cultures used for miRNA arrays (Fig. 3A) or from a biologically distinct donor (Donor 5, Fig. 3B) were differentiated for 7 days using the osteocyte protocol. Osteoblast differentiation was confirmed by testing both sets of cultures for expression of several osteocyte-specific mRNA markers (Fig. 4). The cultures were collected after 7 days of the differentiation protocol, long before most osteoblast markers are significantly increased

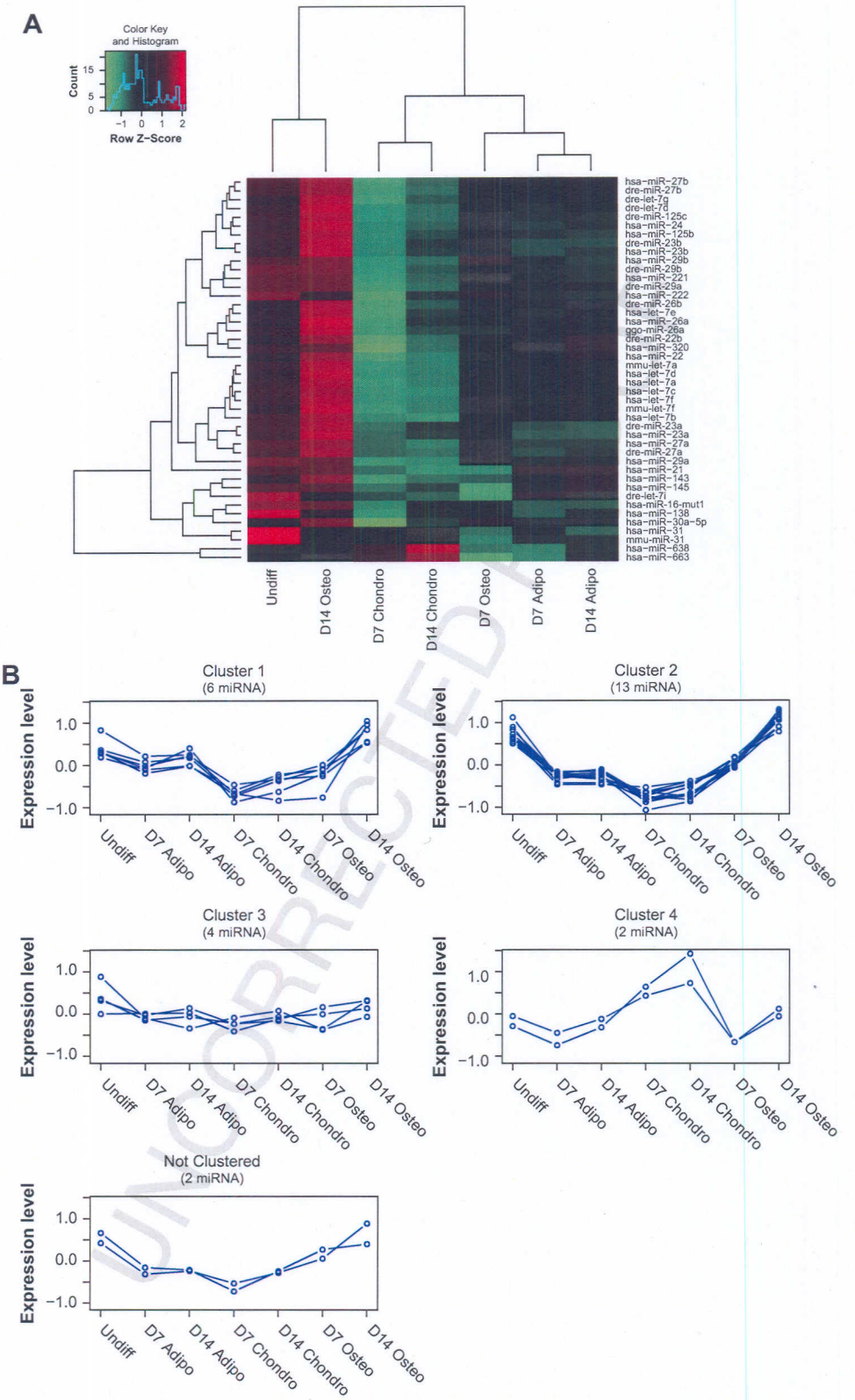

Figure 2. Exploratory microRNA expression patterns in mesenchymal stromal cells (MSC) and differentiating products. A set of pooled MSC were prepared for microRNA analysis on microarrays. (**A**) Hierarchically clustered heatmap of 44 microRNA probes, corresponding to 31 unique mature microRNAs,

(e.g., only alkaline phosphatase, Runx2, and osteopontin are significantly increased for the pooled cultures, and alkaline phosphatase for Donor 5) although all markers exhibit trend toward increased levels in both sets of cultures, demonstrating that the differentiation culture protocol was effective. A comparison between the undifferentiated and differentiated MSCs from either donor source confirms the set of selected osteogenic miRNAs (Clusters 1 and 2 in Fig. 2B; see Table 3 for cluster membership) as significantly regulated during differentiation, and supports the conclusion that these miRNAs are regulated in all MSC by demonstrating their regulation in two separate MSC preparations—one a pool of three donors and one a fourth individual donor. Furthermore, the increased levels of these miRNA markers are uniformly more informative at classifying osteocyte differentiation than the traditional mRNA markers (Fig. 4), confirming our prediction that miRNA changes precede phenotype changes and may be an earlier marker for assessing differentiation in MSC.

Prediction of potential mRNA targets of MSC-associated miRNA

In order to investigate the specific role the PDGF pathway may have on the regulation of miRNAs, we attempted to predict responses to this pathway via bioinformatic analysis of putative promoter regions. Having no specific evidence for the mechanism of transcriptional control of these miRNAs, we hypothesized that genomic sequences upstream of the miRNA coding sites would likely contain regulatory sites responding to PDGF-stimulated transcription factors. Certainly this hypothesis would not be expected to apply to every miRNA, because miRNAs may be expressed intronically [63] for example, but it serves to allow a generalized testing by bioinformatic modeling and pharmacologic manipulation.

A comprehensive literature search identified seven documented downstream effectors of the PDGF pathway (Fig. 5A). Position weight matrices for each of these transcription factors were obtained from the TRANSFAC v11 database [58]. As an approximation of proposed regulatory regions, 5000 base-pair (5 kb) sequences upstream of human miRNA genomic coding sites were collected and scanned for potential PDGF transcription factor–binding sites. As predicted, the collection of MSC-regulated miRNA promoter sequences was enriched for the PDGF-responsive binding sites, possessing significantly more binding site predictions than expressed but unregulated promoters ($p < 0.01$) (Table 2). Thus, the expression of MSC-regulated miRNAs is predicted, as a class, to be regulated by transcription factors within the PDGF pathway.

Next, we sought to identify those individual miRNAs having significantly enriched PDGF response elements. A *Z*-test was used to compare the number of binding sites for each MSC-regulated miRNA against a mean number of binding sites for all 63 expressed miRNAs (Table 3). Using a significance threshold of $p < 0.05$ and a 5% FDR to correct for multiple comparisons, no individual miRNA was found to be enriched for the PDGF pathway. However, we conclude that miRNAs with the lowest probability of satisfying the null hypothesis provide an exploratory confidence list for experimental confirmation. The resulting confidence list is rank-ordered by p value and represents our hypothesized index of miRNAs predicted to be regulated by the PDGF pathway during differentiation of MSCs (Table 3).

Confirmation of PDGF-regulated miRNAs

To test our bioinformatic predictions and to determine the effect of the PDGF-pathway inhibition on the expression of significantly regulated miRNAs, we treated pooled MSCs with the protein tyrosine kinase inhibitor Tyrphostin AG-370 during a 7-day osteogenic differentiation protocol (Fig. 3A), to focus on early miRNA changes and to reduce effects of the long-term toxicity of AG-370 [52]. As hypothesized, the majority of "high-ranking" regulated miRNAs demonstrate significantly reduced expression ($p < 0.05$) in the presence of AG-370 (Fig. 3A; comparisons between differentiated untreated and AG-370-treated). Those miRNAs with predicted responses falling lower on the confidence list showed less of a global reduction in expression upon treatment with the PDGF inhibitor. Pretreatment (48 hours) with AG-370 resulted in a more complex result with several miRNAs responding to pretreatment by exhibiting a reduced expression level, while other miRNAs demonstrated a significant increase upon differentiation, perhaps as a result of a preconditioning effect (results not shown). Regardless, the direct inhibition of PDGF during osteogenic differentiation of MSCs resulted in the reduced expression of several miRNAs.

These results in Figure 3A represent the average response from the four MSC isolates that were pooled in this culture. To test whether predictions would also apply to a biologically distinct MSC isolate, we repeated the AG-370 inhibition study with MSC derived from a single 39-year old male donor (Donor 5, Fig. 3B). As expected, some miRNAs exhibited a different sensitivity to AG-370

identified by testing Hypothesis 1 at 5% % false discovery rate (FDR). The probe list includes nonhuman microRNA sequences, likely due to the inability of hybridization to detect single-nucleotide mismatches in all cases, as described previously [55]. However, similar probes (such as human let-7f and mouse let-7f) cluster similarly and likely detect the same mature human microRNA. Results are color-coded by *Z*-score–normalized expression levels according to the legend and frequency histogram shown as an inset. (**B**) K-means clusters of the 27 unique human microRNAs corresponding to the probes declared significant. From the list of significantly regulated microRNA probes (**A**), unique human mature microRNAs were extracted and clustered using k = 4, which produced the best fit of merit compromise compared with other numbers of clusters tested. Identities of cluster members are shown in Table 3.

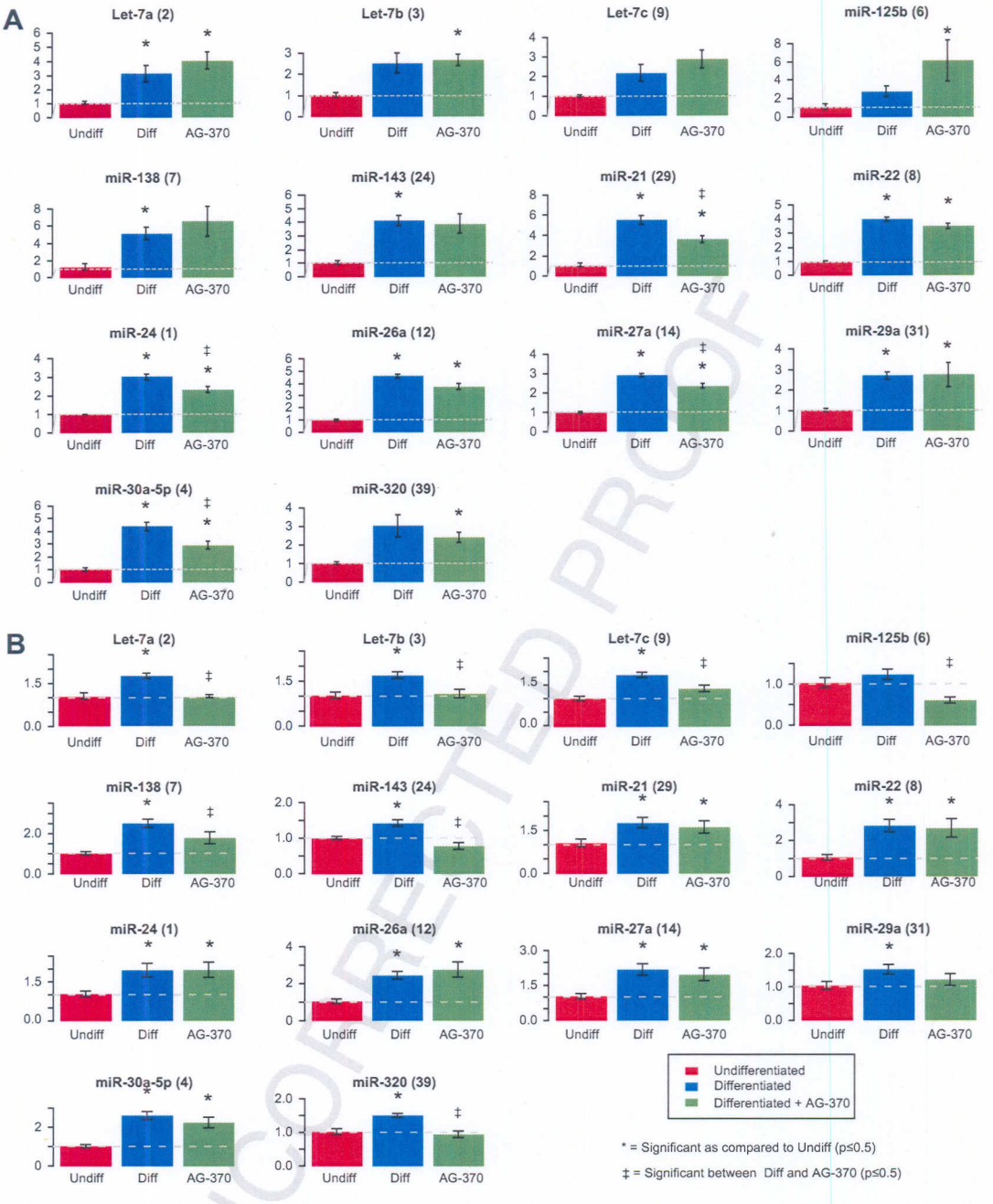

Figure 3. Quantitative polymerase chain reaction (qPCR) assay of microRNAs predicted to be regulated upon osteocyte differentiation or AG-370 treatment. Predictions were tested in either (**A**) pooled mesenchymal stem cell (MSC) cultures identical to those used in the microarrays or (**B**) from a biologically distinct donor (donor 5). In each case, triplicate cultures of MSC were collected as undifferentiated (red bars), differentiated for 7 days following the osteocyte protocol (light blue), or treated with the platelet-derived growth factor (PDGF) pathway inhibitor AG-370 (dark blue) during differentiation. Results depict the mean fold-change from undifferentiated levels, ± standard error of mean (n = 3). To confirm the exploratory microarray results, undifferentiated cultures were compared with differentiated cultures using Student's *t*-test at $p < 0.05$ (*). To confirm predicted regulation by PDGF pathway intermediates, differentiated cultures were compared with AG-370–treated cultures by Student's *t*-test at $p < 0.05$ (‡). For each microRNA assay, the rank position in the confidence list (**Table 3**) is shown in parentheses.

inhibition, however, the majority of miRNAs ranking highly on the prediction list (**Table 3**) were similarly inhibited in each cell preparation. We conclude that PDGF mediation of miRNA regulation, whether due to a direct or indirect mechanism, is a general feature of MSC differentiation into osteoblasts and may play a role in promoting differentiation. More importantly, pathway analysis of miRNA expression patterns during MSC differentiation

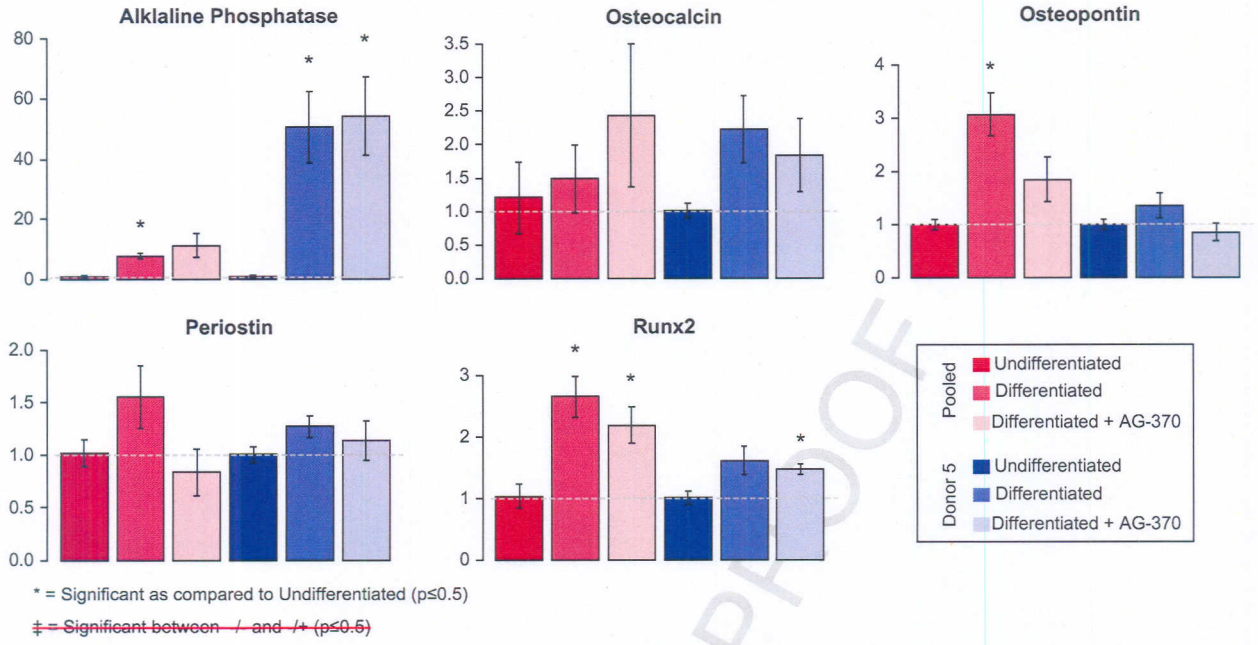

Figure 4. Confirmation of osteocyte phenotype upon differentiation of mesenchymal stem cell (MSC) cultures. Pooled donor MSC cultures (red) or individual donor 5 cultures (blue) were assayed for osteocyte marker mRNAs after 7 days of differentiation by quantitative polymerase chain reaction. Mean ± standard error of mean (n = 3 cultures) values of RQ (relative quantities, based on glyceraldehyde 3-phosphate dehydrogenase (GAPDH) internal control mRNA and undifferentiated cultures using the $\Delta\Delta C_t$ method). Differences were tested using Student's *t*-test and are marked with an asterisk (*) as increased from undifferentiated ~~or a dagger (‡) as decreased with AG 370 treatment from differentiated~~ at $p < 0.05$.

yields interpretable results that may be tested using standard biochemical techniques.

Discussion

Our goal was not only to identify miRNAs that are regulated during differentiation of MSC but also to predict a subset of miRNAs that could be regulated by a specific signaling pathway. As an example, we chose the PDGF signaling pathway and its regulated transcription factors (Fig. 5A). By measuring the frequency of finding transcription factor binding sites (using position weight matrices from the TRANSFAC database) within 2-kb upstream of mature miRNA on the genome, and comparing frequencies between miRNAs regulated during osteogenesis with those that are not regulated, we identified a set of putatively PDGF-regulated miRNAs. To test this prediction, we inhibited PDGF signaling during osteogenic differentiation and found that many of the predicted miRNAs are affected (Fig. 3). This leads to our hypothesized regulatory network, as depicted in Figure 5B. PDGF signaling would be expected to regulate a target set of transcription factors, among other genes [52]. In addition to downstream regulation of target mRNAs, these PDGF-regulated transcription factors may also regulate miRNA transcription. The resulting miRNAs would be predicted to inhibit, for example, nonosteogenic mRNA translation, reinforcing the regulatory network. By predicting PDGF-regulated miRNAs and then confirming the involvement of PDGF in their regulation, we have laid the initial groundwork to support this novel network in osteogenic differentiation.

In general, the multilineage differentiation potential and the possibility of using an autologous source of MSC isolated from patient bone marrow makes it an appealing and promising cell therapy agent for treating various human diseases [10]. Generating sufficient amounts of cells for therapeutic application requires extensive culture of MSC in vitro starting from the bone marrow [5]. Several methods of expansion and maintenance resulting in MSC with varying differentiation potential have been reported [64–66]. To promote these cells as routine clinical agents, more detailed characterization of the molecular regulatory network level is necessary.

We characterized individual and/or pooled MSC using cell sorting of surface markers (Fig. 1A), cytochemistry of differentiated cultures (Fig. 1B), and a comprehensive screen of the gene expression and miRNA expression patterns of MSC and the changes that occur upon differentiation into adipocytes or osteocytes (Fig. 1C, Table 1, Suppl. Table 1). Samples used for expression analysis were similar in their proliferative potential, based on their population doubling time (not shown), and differentiation potential, based on morphology and staining pattern of differentiated cells. Gene expression profiling demonstrated several sources of variability among MSC isolates, but it readily distinguished them from other pluripotent

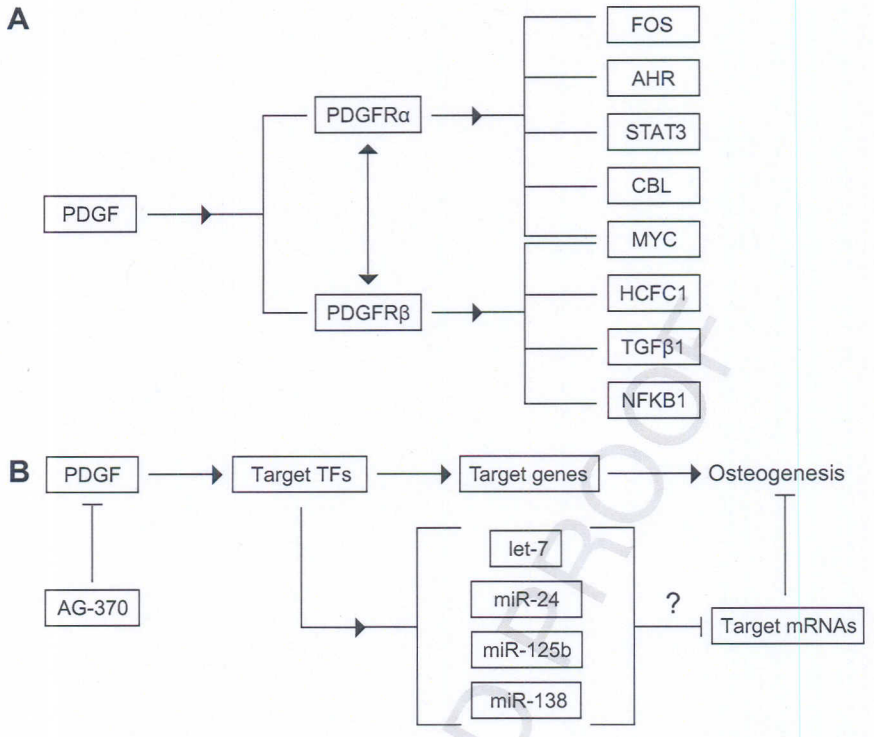

Figure 5. Regulatory networks in mesenchymal stem cell (MSC) differentiation. (**A**) Platelet-derived growth factor (PDGF)–responsive pathways leading to regulation of transcription factors. This pathway was assembled using Pathway Architect (Stratagene) to identify potentially regulated transcription factors likely to be affected by PDGF receptor stimulation. Each pathway is supported by at least one publication from the scientific literature (not shown). (**B**) Proposed regulatory network. PDGF signaling, inhibited by Tyrphostin AG-370, induces specific transcription factors [identified in (**A**)], in turn regulating both osteogenic target mRNA genes and a specific set of microRNAs, including let-7, miR-24, miR-125b, and miR-138. Increased levels of those microRNAs are predicted to inhibit translation of non-osteogenic target mRNAs to diminish their inhibition of osteogenesis.

cell types such as ESC [67]. MSC are heterogeneous populations of cells. MCS are derived from different tissue sources and different donors, leading to a high degree of variability between isolates, as demonstrated by the correlation studies in Supplemental Figure 1. Furthermore, unlike most ESC, the same MSC cell line can vary with passage, adding to the difficulty in describing these cultures with gene expression. Demonstrating with this issue, the correlation value between one donor-derived MSC was somewhat different from another, indicating basal differences in donor MSC (e.g., R^2 of 0.912 between MSC from two donors in Suppl. Fig. 1E). A similar deviation was also observed with the same donor MSC, but differing by one passage with variation largely resulting from low-level expression of genes (0.804, Suppl. Fig. 1F). The correlation value of MSC and differentiated progeny was much lower, indicating a greater deviation in the global gene expression profile upon differentiation. In spite of the differences between the various MSC populations, we were able to select a consistent set of genes for which the change in pattern of expressed gene between undifferentiated MSC and cells differentiated to adipocytes or osteocytes tightly cluster indicating the overall similarity between the cell groups (Suppl. Fig. 1B).

The role of miRNA expression as a key regulatory element in differentiation is recognized but is still poorly defined at the level of specific mechanisms. Interestingly, the pattern of miRNA expression in MSC is substantially different from pluripotent stem cells such as human embryonal carcinoma and human ESC [49,50]. Known pluripotent associated markers such as miR302a, b, c and d, and miR 200c are absent in MSC (see Table 3). Again, despite the heterogeneous nature of MSC, a group of miRNAs was identified as differentially expressed between MSCs, differentiated adipocytes, chondrocytes, and osteocytes.

Collection of both miRNA and mRNA gene expression patterns enables us to begin to examine specific cellular mechanisms or pathway regulated during MSC differentiation. As an example of this approach, we describe the predicted regulation of a set of miRNAs by members of the PDGF pathway, which was previously identified through pathway analysis of MSC gene expression results [52]. While PDGF is not normally known as a mediator of osteogenic differentiation, the addition of AG-370 reduced the number of osteocytes and mineralization [52]. It remains possible that inhibition of PDGF has an indirect effect on osteogenic differentiation through reduced proliferation, but this would also require activation of intracellular signaling. We were

Table 2. Frequency of position weight matrix hits specific for PDGF pathway in expressed but not regulated microRNAs vs regulated microRNAs

		Nonregulated		Regulated	
Transcription factor	Matrix Identifier	Hits	Hits/miRNA	Hits	Hits/miRNA
AhR	V$AHR_01	11	0.46	15	0.38
	V$AHR_Q5	1	0.04	1	0.03
	V$AHRARNT_01	2	0.08	7	0.18
	V$AHRARNT_02	1	0.04	13	0.33
	V$AHRHIF_Q6	0	0.00	17	0.44
Jun(2)/AP1	V$AP1_01	38	1.58	83	2.13
	V$AP1_Q2_01	9	0.38	21	0.54
	V$AP1_Q4_01	1	0.04	6	0.15
	V$AP1_Q6_01	7	0.29	13	0.33
	V$AP1FJ_Q2	6	0.25	11	0.28
NFKB1	V$EBOX_Q6_01	9	0.38	26	0.67
Myc	V$MYC_Q2	10	0.42	44	1.13
	V$MYCMAX_01	0	0.00	18	0.46
	V$MYCMAX_02	1	0.04	4	0.10
	V$MYCMAX_B	1	0.04	0	0.00
	V$NMYC_01	0	0.00	5	0.13
STAT3	V$STAT_01	6	0.25	7	0.18
	V$STAT_Q6	13	0.54	21	0.54
	V$STAT3_01	7	0.29	4	0.10
	V$STAT3_02	9	0.38	25	0.64

To test whether potentially platelet-derived growth factor (PDGF)–responsive DNA sequences could be found within a genomic region 5-kb upstream of microRNAs (miRNAs) regulated during osteogenesis, we counted the number of "hits" or sequences matching the position weight matrix (PWM) describing all variations of a known transcription factor binding site. The TRANSFAC matrix identifier is listed for each PWM matching a PDGF pathway transcription factor (summarized in **Fig. 5**A). Two groups of results are shown for nonregulated miRNA that were found to be expressed in MSC and differentiated products and for miRNAs selected as significantly regulated (see **Fig. 2** and **Table 3**).

able to confirm involvement of this specific pathway in the osteogenic differentiation of MSCs. We then successfully determined that genes in this pathway have a greater likelihood of regulating miRNAs identified as significant from the same samples, based on the content of their upstream sequences (**Table 3**). While we were unable to statistically predict specific miRNAs having an enriched presence of PDGF-responsive binding sites, we were able to demonstrate good concordance between an exploratory ranking (**Table 3**) and results of PDGF pathway inhibition using AG-370 in both pooled MSCs (**Fig. 3**A) and a biologically distinct MSC preparation (**Fig. 3**B). In another example of PDGF involvement with miRNAs, mir-140 was found to inhibit PDGF signaling in zebrafish, helping to control formation of palate [68], demonstrating a complementary relationship in a developmental program other than MSC. Together, these studies demonstrate how existing network information can be applied in conjunction with miRNA expression data to begin to unravel the as yet elusive mechanisms governing the regulation of these small molecules.

A second benefit to this approach is realized when we examine the target predictions using regulated mRNAs and miRNAs to generate hypotheses for future analyses. These associations are abundant across our two datasets. For example, SLC7A5 is predicted by the RNA22 algorithm [69] to be targeted by mir-26A, which increases in adipocytes. However, SLC7A5 mRNA increases in both adipocytes and osteoblasts, and this mRNA is not normally found in adult adipocytes, but is found in bone. Perhaps the adipocyte-specific transcriptional regulation of SLC7A5 is not yet active and the miRNA inhibition of expression shifts the cell away from bone phenotype. Another example, STARD8, is similarly expressed in bone but not adipose tissue. This mRNA is increased during both adipocyte and osteoblast differentiation over MSC and is predicted to be targeted by mir-31. Because mir-31 is not reduced in adipocytes, does this inhibitory mechanism prevent production of STARD8 in adipocytes?

Transcription factors are likely to participate in differentiation mechanisms. GATA6, known to be involved in cardiac and lung differentiation [70], is increased in osteoblasts compared with MSC but not in adipocytes. Because mir-31 continues to be expressed in adipocytes, this may be a mechanism for inhibiting continued expression of GATA6 as MSC differentiate into adipocytes. ARNT2, an aryl hydrocarbon nuclear translocator protein known to be expressed in bone stromal cells [71] is another target of mir-31 that may be inhibited in adipocytes. ARNT2 may be derepressed because mir-31 decreases in osteoblasts. The majority of these predictions focus on mir-31 as a likely inhibitor of the osteocyte differentiation pathway and a good candidate for knockdown in future experiments.

While variability in the miRNA expression between MSC derived from different donors is apparent both in its

Table 3. Ranking of individual microRNAs by relative frequencies of transcription-factor binding sites

miRNA Precursor	Mature miRNA	K-means cluster	*p* Value	Rank (i)	FDR Cut-off
hsa-mir-24-1	hsa-miR-24	2	0.002	1	0.001
hsa-let-7a-3	hsa-let-7a	2	0.003	2	0.003
hsa-let-7b	hsa-let-7b	2	0.009	3	0.004
hsa-mir-30a	hsa-mir-30a	3	0.069	4	0.005
has-mir-31	has-mir-31	3	0.095	5	0.006
hsa-mir-125b-2	hsa-mir-125b	2	0.129	6	0.008
hsa-mir-138-1	hsa-mir-138	3	0.129	7	0.009
hsa-mir-22	hsa-mir-22	1	0.129	8	0.010
hsa-let-7c	hsa-let-7c	2	0.160	9	0.012
hsa-let-7 g	hsa-let-7 g	2	0.160	10	0.013
hsa-mir-16-1	hsa-mir-16	3	0.160	11	0.014
hsa-mir-26a-2	hsa-mir-26a	2	0.210	12	0.015
hsa-mir-23a	hsa-mir-23a	2	0.220	13	0.017
hsa-mir-27a	hsa-mir-27a	2	0.220	14	0.018
hsa-mir-27b	hsa-mir-27b	2	0.220	15	0.019
hsa-let-7i	hsa-let-7i	2	0.260	16	0.021
hsa-mir-26a-1	hsa-mir-26a	2	0.260	17	0.022
hsa-mir-24-2	hsa-mir-24	2	0.270	18	0.023
hsa-mir-638	hsa-mir-638	4	0.270	19	0.024
hsa-let-7a-1	hsa-let-7a	2	0.320	20	0.026
hsa-let-7a-2	hsa-let-7a	2	0.320	21	0.027
hsa-let-7f-1	hsa-let-7f	2	0.320	22	0.028
hsa-mir-125b-1	hsa-mir-125b	2	0.320	23	0.029
hsa-mir-143	hsa-mir-143	1	0.320	24	0.031
hsa-mir-16-2	hsa-mir-16	3	0.320	25	0.032
hsa-let-7d	hsa-let-7d	2	0.330	26	0.033
hsa-mir-23b	hsa-mir-23b	2	0.340	27	0.035
hsa-mir-29b-2	hsa-mir-29b	2	0.340	28	0.036
hsa-mir-21	hsa-mir-21	1	0.390	29	0.037
hsa-mir-222	hsa-mir-222	5	0.390	30	0.038
hsa-mir-29a	hsa-mir-29a	2	0.390	31	0.040
hsa-mir-29b-1	hsa-mir-29b	2	0.390	32	0.041
hsa-mir-138-2	hsa-mir-138	3	0.400	33	0.042
hsa-mir-145	hsa-mir-145	3	0.400	34	0.044
hsa-mir-663	hsa-mir-663	4	0.410	35	0.045
hsa-let-7f-2	hsa-let-7f	2	0.420	36	0.046
hsa-let-7e	hsa-let-7e	1	0.460	37	0.047
hsa-mir-221	hsa-mir-221	2	0.460	38	0.049
hsa-mir-320	hsa-mir-320	1	0.470	39	0.050

Each unique human microRNA (miRNA) genomic locus (identified by precursor name) is associated with the name of the mature microRNA, the K-means cluster ID (**Fig. 2**B), the *z*-score *p* value, the rank of the *p* value, and the Benjamini-Hochberg **[60]** false discovery (FDR) rate cut-off. The *z*-score *p* value is calculated by comparing the number of position weight matrix matches within this 5-kb region upstream of each miRNA genomic locus with the average match rate for all for regulated and non-regulated miRNA loci. The false discovery rate cut-off lists the *p* value that would be within the 5% FDR level if this ranked p-value were less than the cutoff. Therefore, no individual miRNA locus was judged to be significant compared with all expressed miRNA loci. However, the resulting, rank-ordered list highlights miRNAs having a greater chance of being regulated by platelet-derived growth factor (PDGF) at the top and least likely to be regulated by PDGF at the bottom.

undifferentiated state and cells differentiated to adipocytes or osteoblast, the pattern of miRNA expression is distinct from earlier reported expression in human embryonic stem cells and their differentiated cells. Combined analysis of miRNAs and mRNAs expression in heterogeneous stem cell populations such as MSC provides a tool to identify possible miRNA regulators and their gene targets providing a rationale for further perturbation studies.

Acknowledgments

R.P.H. was supported by grants from the New Jersey Commission on Spinal Cord Research, the New Jersey Commission on Science and Technology, National Institutes of Health, and Invitrogen, Inc. C.R. was supported by a National Science Foundation IGERT fellowship. U.L. thanks Mark Landers, Invitrogen, for his support and help with initial NCode miRNA array and qPCR analysis.

References

1. Noth U, Osyczka AM, Tuli R, Hickok NJ, Danielson KG, Tuan RS. Multilineage mesenchymal differentiation potential of human trabecular bone-derived cells. J Orthop Res. 2002;20:1060–1069.
2. Tuan RS, Boland G, Tuli R. Adult mesenchymal stem cells and cell-based tissue engineering. Arthritis Res Ther. 2003;5:32–45.
3. Sarugaser R, Lickorish D, Baksh D, Hosseini MM, Davies JE. Human umbilical cord perivascular (HUCPV) cells: a source of mesenchymal progenitors. Stem Cells. 2005;23:220–229.
4. Caplan AI. Mesenchymal stem cells. J Orthop Res. 1991;9:641–650.
5. Pittenger MF, Mackay AM, Beck SC, et al. Multilineage potential of adult human mesenchymal stem cells. Science. 1999;284:143–147.
6. Gronthos S, Graves SE, Ohta S, Simmons PJ. The STRO-1+ fraction of adult human bone marrow contains the osteogenic precursors. Blood. 1994;84:4164–4173.
7. Minguell JJ, Erices A, Conget P. Mesenchymal stem cells. Exp Biol Med (Maywood). 2001;226:507–520.
8. Tocci A, Forte L. Mesenchymal stem cell: use and perspectives. Hematol J. 2003;4:92–96.
9. Bianchi G, Banfi A, Mastrogiacomo M, et al. Ex vivo enrichment of mesenchymal cell progenitors by fibroblast growth factor 2. Exp Cell Res. 2003;287:98–105.
10. Bianco P, Riminucci M, Gronthos S, Robey PG. Bone marrow stromal stem cells: nature, biology, and potential applications. Stem Cells. 2001;19:180–192.
11. Colter DC, Class R, DiGirolamo CM, Prockop DJ. Rapid expansion of recycling stem cells in cultures of plastic-adherent cells from human bone marrow. Proc Natl Acad Sci U S A. 2000;97:3213–3218.
12. Awad HA, Butler DL, Boivin GP, et al. Autologous mesenchymal stem cell-mediated repair of tendon. Tissue Eng. 1999;5:267–277.
13. Bruder SP, Jaiswal N, Haynesworth SE. Growth kinetics, self-renewal, and the osteogenic potential of purified human mesenchymal stem cells during extensive subcultivation and following cryopreservation. J Cell Biochem. 1997;64:278–294.
14. Bruder SP, Kurth AA, Shea M, Hayes WC, Jaiswal N, Kadiyala S. Bone regeneration by implantation of purified, culture-expanded human mesenchymal stem cells. J Orthop Res. 1998;16:155–162.
15. Dennis JE, Merriam A, Awadallah A, Yoo JU, Johnstone B, Caplan AI. A quadripotential mesenchymal progenitor cell isolated from the marrow of an adult mouse. J Bone Miner Res. 1999;14:700–709.
16. Ferrari G, Cusella-De Angelis G, Coletta M, et al. Muscle regeneration by bone marrow-derived myogenic progenitors. Science. 1998;279:1528–1530.
17. Galmiche MC, Koteliansky VE, Briere J, Herve P, Charbord P. Stromal cells from human long-term marrow cultures are mesenchymal cells that differentiate following a vascular smooth muscle differentiation pathway. Blood. 1993;82:66–76.

18. Prockop DJ. Marrow stromal cells as stem cells for nonhematopoietic tissues. Science. 1997;276:71–74.
19. Young RG, Butler DL, Weber W, Caplan AI, Gordon SL, Fink DJ. Use of mesenchymal stem cells in a collagen matrix for Achilles tendon repair. J Orthop Res. 1998;16:406–413.
20. Dormady SP, Bashayan O, Dougherty R, Zhang XM, Basch RS. Immortalized multipotential mesenchymal cells and the hematopoietic microenvironment. J Hematother Stem Cell Res. 2001;10:125–140.
21. Gronthos S, Zannettino AC, Hay SJ, et al. Molecular and cellular characterisation of highly purified stromal stem cells derived from human bone marrow. J Cell Sci. 2003;116:1827–1835.
22. Kuznetsov SA, Krebsbach PH, Satomura K, et al. Single-colony derived strains of human marrow stromal fibroblasts form bone after transplantation in vivo. J Bone Miner Res. 1997;12:1335–1347.
23. Majumdar MK, Thiede MA, Mosca JD, Moorman M, Gerson SL. Phenotypic and functional comparison of cultures of marrow-derived mesenchymal stem cells (MSCs) and stromal cells. J Cell Physiol. 1998; 176:57–66.
24. Muraglia A, Cancedda R, Quarto R. Clonal mesenchymal progenitors from human bone marrow differentiate in vitro according to a hierarchical model. J Cell Sci. 2000;113(Pt 7):1161–1166.
25. Osyczka AM, Noth U, O'Connor J, et al. Multilineage differentiation of adult human bone marrow progenitor cells transduced with human papilloma virus type 16 E6/E7 genes. Calcif Tissue Int. 2002;71:447–458.
26. Horwitz EM, Gordon PL, Koo WK, et al. Isolated allogeneic bone marrow-derived mesenchymal cells engraft and stimulate growth in children with osteogenesis imperfecta: Implications for cell therapy of bone. Proc Natl Acad Sci U S A. 2002;99:8932–8937.
27. Koc ON, Gerson SL, Cooper BW, et al. Rapid hematopoietic recovery after coinfusion of autologous-blood stem cells and culture-expanded marrow mesenchymal stem cells in advanced breast cancer patients receiving high-dose chemotherapy. J Clin Oncol. 2000;18:307–316.
28. Petite H, Viateau V, Bensaid W, et al. Tissue-engineered bone regeneration. Nat Biotechnol. 2000;18:959–963.
29. Doi M, Nagano A, Nakamura Y. Molecular cloning and characterization of a novel gene, EMILIN-5, and its possible involvement in skeletal development. Biochem Biophys Res Commun. 2004;313:888–893.
30. Qi H, Aguiar DJ, Williams SM, La Pean A, Pan W, Verfaillie CM. Identification of genes responsible for osteoblast differentiation from human mesodermal progenitor cells. Proc Natl Acad Sci U S A. 2003;100:3305–3310.
31. Chen CZ, Li L, Lodish HF, Bartel DP. MicroRNAs modulate hematopoietic lineage differentiation. Science. 2004;303:83–86.
32. Chen CZ, Lodish HF. MicroRNAs as regulators of mammalian hematopoiesis. Semin Immunol. 2005;17:155–165.
33. Esau C, Kang X, Peralta E, et al. MicroRNA-143 regulates adipocyte differentiation. J Biol Chem. 2004;279:52361–52365.
34. Hatfield SD, Shcherbata HR, Fischer KA, Nakahara K, Carthew RW, Ruohola-Baker H. Stem cell division is regulated by the microRNA pathway. Nature. 2005;435:974–978.
35. Kuwabara T, Hsieh J, Nakashima K, Taira K, Gage FH. A small modulatory dsRNA specifies the fate of adult neural stem cells. Cell. 2004; 116:779–793.
36. Wu L, Belasco JG. Micro-RNA regulation of the mammalian lin-28 gene during neuronal differentiation of embryonal carcinoma cells. Mol Cell Biol. 2005;25:9198–9208.
37. Zhao Y, Samal E, Srivastava D. Serum response factor regulates a muscle-specific microRNA that targets Hand2 during cardiogenesis. Nature. 2005;436:214–220.
38. Calin GA, Sevignani C, Dumitru CD, et al. Human microRNA genes are frequently located at fragile sites and genomic regions involved in cancers. Proc Natl Acad Sci U S A. 2004;101:2999–3004.
39. Cheng AM, Byrom MW, Shelton J, Ford LP. Antisense inhibition of human miRNAs and indications for an involvement of miRNA in cell growth and apoptosis. Nucleic Acids Res. 2005;33:1290–1297.
40. Yu Z, Raabe T, Hecht NB. MicroRNA Mirn122a reduces expression of the posttranscriptionally regulated germ cell transition protein 2 (Tnp2) messenger RNA (mRNA) by mRNA cleavage. Biol Reprod. 2005;73:427–433.
41. Sullivan CS, Ganem D. MicroRNAs and viral infection. Mol Cell. 2005;20:3–7.
42. Berezikov E, Guryev V, van de Belt J, Wienholds E, Plasterk RH, Cuppen E. Phylogenetic shadowing and computational identification of human microRNA genes. Cell. 2005;120:21–24.
43. Houbaviy HB, Murray MF, Sharp PA. Embryonic stem cell-specific MicroRNAs. Dev Cell. 2003;5:351–358.
44. Kanellopoulou C, Muljo SA, Kung AL, et al. Dicer-deficient mouse embryonic stem cells are defective in differentiation and centromeric silencing. Genes Dev. 2005;19:489–501.
45. Murchison EP, Partridge JF, Tam OH, Cheloufi S, Hannon GJ. Characterization of Dicer-deficient murine embryonic stem cells. Proc Natl Acad Sci U S A. 2005;102:12135–12140.
46. Suh MR, Lee Y, Kim JY, et al. Human embryonic stem cells express a unique set of microRNAs. Dev Biol. 2004;270:488–498.
47. Tang F, Hajkova P, Barton SC, Lao K, Surani MA. MicroRNA expression profiling of single whole embryonic stem cells. Nucleic Acids Res. 2006;34: e9.
48. Yang S, Tutton S, Pierce E, Yoon K. Specific double-stranded RNA interference in undifferentiated mouse embryonic stem cells. Mol Cell Biol. 2001;21:7807–7816.
49. Josephson R, Ording CJ, Liu Y, et al. Qualification of embryonal carcinoma 2102ep as a reference for human embryonic stem cell research. Stem Cells. 2007;25:437–446.
50. ~~Lakshmipathy U, Love B, Goff L, et al. Micro RNA expression pattern of undifferentiated and differentiated human embryonic stem cells. Stem Cells Dev. In press.~~ Q14
51. Wang Y, Medvid R, Melton C, Jaenisch R, Blelloch R. DGCR8 is essential for microRNA biogenesis and silencing of embryonic stem cell self-renewal. Nat Genet. 2007;39:380–385.
52. ~~Ng F, Boucher S, Koh S, et al. PDGF, TGF-b and FGF signaling is important for differentiation and growth of mesenchymal stem cells (MSCs): transcriptional profiling can identify markers and signaling pathways important in differentiation of MSC into adipogenic, chondrogenic and osteogenic lineages. Blood; 2008.~~ Q15
53. Liu Y, Shin S, Zeng X, et al. Genome wide profiling of human embryonic stem cells (hESCs), their derivatives and embryonal carcinoma cells to develop base profiles of U.S. Federal government approved hESC lines. BMC Dev Biol. 2006;6:20.
54. Kerr MK, Martin M, Churchill GA. Analysis of variance for gene expression microarray data. J Comput Biol. 2000;7:819–837.
55. Goff LA, Yang M, Bowers J, Getts RC, Padgett RW, Hart RP. Rational probe optimization and enhanced detection strategy for microRNAs using micorarrays. RNA Biol. 2005;2:e9–e616.
56. Lakshmipathy U, Love B, Adams C, Thyagarajan B, Chesnut JD. MicroRNA profiling: an easy and rapid method to screen and characterize stem cell populations. In: Vemuri MC, ed. Stem cell assays. Clifton, NJ: Humana Press; 2006.
57. Kerr MK, Churchill GA. Experimental design for gene expression microarrays. Biostatistics. 2001;2:183–201.
58. Matys V, Fricke E, Geffers R, et al. TRANSFAC: transcriptional regulation, from patterns to profiles. Nucleic Acids Res. 2003;31:374–378.
59. Dominici M, Le Blanc K, Mueller I, et al. Minimal criteria for defining multipotent mesenchymal stromal cells. The International Society for Cellular Therapy position statement. Cytotherapy. 2006;8:315–317.
60. Benjamini Y, Hochberg Y. Controlling the false discovery rate—a practical and powerful approach to multiple testing. J R Stat Soc Ser B Method. 1995;57:289.
61. Kratchmarova I, Blagoev B, Haack-Sorensen M, Kassem M, Mann M. Mechanism of divergent growth factor effects in mesenchymal stem cell differentiation. Science. 2005;308:1472–1477.

62. Nimura A, Muneta T, Koga H, et al. Increased proliferation of human synovial mesenchymal stem cells with autologous human serum: comparisons with bone marrow mesenchymal stem cells and with fetal bovine serum. Arthritis Rheum. 2008;58:501–510.
63. Ying SY, Lin SL. Intronic microRNAs. Biochem Biophys Res Commun. 2005;326:515.
64. Meuleman N, Tondreau T, Delforge A, et al. Human marrow mesenchymal stem cell culture: serum-free medium allows better expansion than classical alpha-MEM medium. Eur J Haematol. 2006;76:309–316.
65. Sotiropoulou PA, Perez SA, Salagianni M, Baxevanis CN, Papamichail M. Characterization of the optimal culture conditions for clinical scale production of human mesenchymal stem cells. Stem Cells. 2006; 24:462–471.
66. Muller I, Kordowich S, Holzwarth C, et al. Animal serum-free culture conditions for isolation and expansion of multipotent mesenchymal stromal cells from human BM. Cytotherapy. 2006;8:437–444.
67. Cai J, Chen J, Liu Y, et al. Assessing self-renewal and differentiation in human embryonic stem cell lines. Stem Cells. 2006;24:516–530.
68. Eberhart JK, He X, Swartz ME, et al. MicroRNA Mirn140 modulates Pdgf signaling during palatogenesis. Nat Genet. 2008;40:290–298.
69. Miranda KC, Huynh T, Tay Y, et al. A pattern-based method for the identification of MicroRNA binding sites and their corresponding heteroduplexes. Cell. 2006;126:1203–1217.
70. Morrisey EE, Ip HS, Lu MM, Parmacek MS. GATA-6: a zinc finger transcription factor that is expressed in multiple cell lineages derived from lateral mesoderm. Dev Biol. 1996;177:309–322.
71. Lavin AL, Hahn DJ, Gasiewicz TA. Expression of functional aromatic hydrocarbon receptor and aromatic hydrocarbon nuclear translocator proteins in murine bone marrow stromal cells. Arch Biochem Biophys. 1998;352:9–18.
72. Stroncek DF, Jin P, Wang E, Jett B. Potency analysis of cellular therapies: the emerging role of molecular assays. J Transl Med. 2007;5:24.

Supplemental methods

Illumina microarray data analysis methods

To include sources of biological variability as well as to gain statistical power, four replicates consisting of three individual donor samples cultured at several different passages (donor 1, passage 7 or 8; donor 2 passage 10, donor 3 passage 10), differentiated as described previously, were hybridized to Illumina Bead arrays. The overall signal intensity distributions obtained on the Illumina arrays were used as a measure of array quality and this distribution did not vary materially among the samples assayed, confirming the technical quality of this analysis.

To focus on expressed genes, we first selected detected genes having a confidence of ≥0.95 in at least 50% of the samples, resulting in 12,414 out of 47,289 genes. We applied quantile normalization to these data, and we then calculated the relatedness between samples using Pearson correlation as the metric and again displayed results as a hierarchically clustered dendrogram (Suppl. Fig. 1A). Results demonstrate a generally accurate clustering by cell type (see the relatively tight grouping of the osteocyte group), but also indicate the high degree of variability between donors (see the split among the adipocytes from different donors), although, unlike our miRNA measurements on individual donors, there was sufficient similarity within groups to identify cell type–specific mRNA regulation. A major component of the variability between samples is a group of genes that are expressed at similar levels in all conditions, for example, 1090 genes had mean levels within 25% of identity across all three cell types among 6947 exhibiting expression above the minimum confidence level in at least one cell group and not selected by analysis of variance.

To test the level of similarity in gene expression between each combination of samples, pairwise correlations were calculated for each of the undifferentiated MSC and their differentiated cell types (demonstrated in selected scatter plots, Suppl. Fig. 1C – F). The correlation values suggest that the extent of specific gene expression differs even at the basal level between MSC samples from these two donors, though this was relatively minimal compared to differences between MSC and their differentiated progeny. Additionally, these results indicate general consistency among MSC prepared from different donors and a greater difference between MSC and differentiated products.

NCode microarray data analysis methods

The microarray analysis of variance package in R (http://www.r-project.org/) was used to analyze miRNA expression between undifferentiated mesenchymal stem cells and its differentiated progeny. Raw array data were log transformed ($\log_2$) and fit to a linear model that calculates the main effects and interactions found in the following equation [72]:

$$y_{ijkg} = \mu + A_i + D_j + V_k + G_g + (VG)_{kg} + (AG)_{ig} + \epsilon_{ijkg}$$

The advantage to using such a model is that it allows differences in gene expression to be isolated to different factors, which can then be used to estimate the overall effect of being array i, dye j, sample k, and gene g. The effect of interest is the interaction of gene and sample (VG). This effect identifies differences in miRNA expression across the different samples. The microarray analysis of variance package fit the raw array data to the linear model twice, once including the VG effects and once without the VG effects. By comparing these two linear fits, the VG interaction could be analyzed using an F-test. A p value for each miRNA was obtained by bootstrapping 10,000 permutations of the fitted data. Significant microRNAs were selected at $p < 0.05$ and having a FDR of 5%.

To identify miRNAs regulated during MSC differentiation, we designed our analyses to test two hypotheses. The first analysis was designed to look for any significant differences in gene expression between samples, thus testing:
Hypothesis 1

H_o: U = 7A = 7C = 7O = 14A = 14C = 14O
H_1: U ≠ 7A ≠ 7C ≠ 7O ≠ 14A ≠ 14C ≠ 14O
(U = Undifferentiated MSC, A = Adipocytes,
C = Chondrocytes, O = Osteocytes,
7= Day 7, 14 = Day 14)

The second analysis was designed to confirm osteocyte-specific miRNAs, comparing the miRNA expression of day 7 and 14 osteocytes to all other samples. This analysis looked for differences between osteocytes and nonosteocytes, thus testing:
Hypothesis 2

H_o: Osteo = Non-Osteo
H_2: Osteo ≠ Non-Osteo
(Osteo = 7O & 14O; Non-Osteo = U, 7A, 7C, 14A, & 14C)

Supplement Table 1. The 1384 probes for gene transcripts selected by analysis of variance analysis
Table is downloadable from:
http://cord.rutgers.edu/appendix/msc/Supplemental_Table_1.xls
Asterisks identify membership in each of the post-hoc lists. Signal intensity values are quantile normalized. Predicted microRNA targets are listed if a matching prediction is found in the downloaded RNA22 database [69] using ENSEMBL transcript IDs derived from BIOMART to match mRNAs.

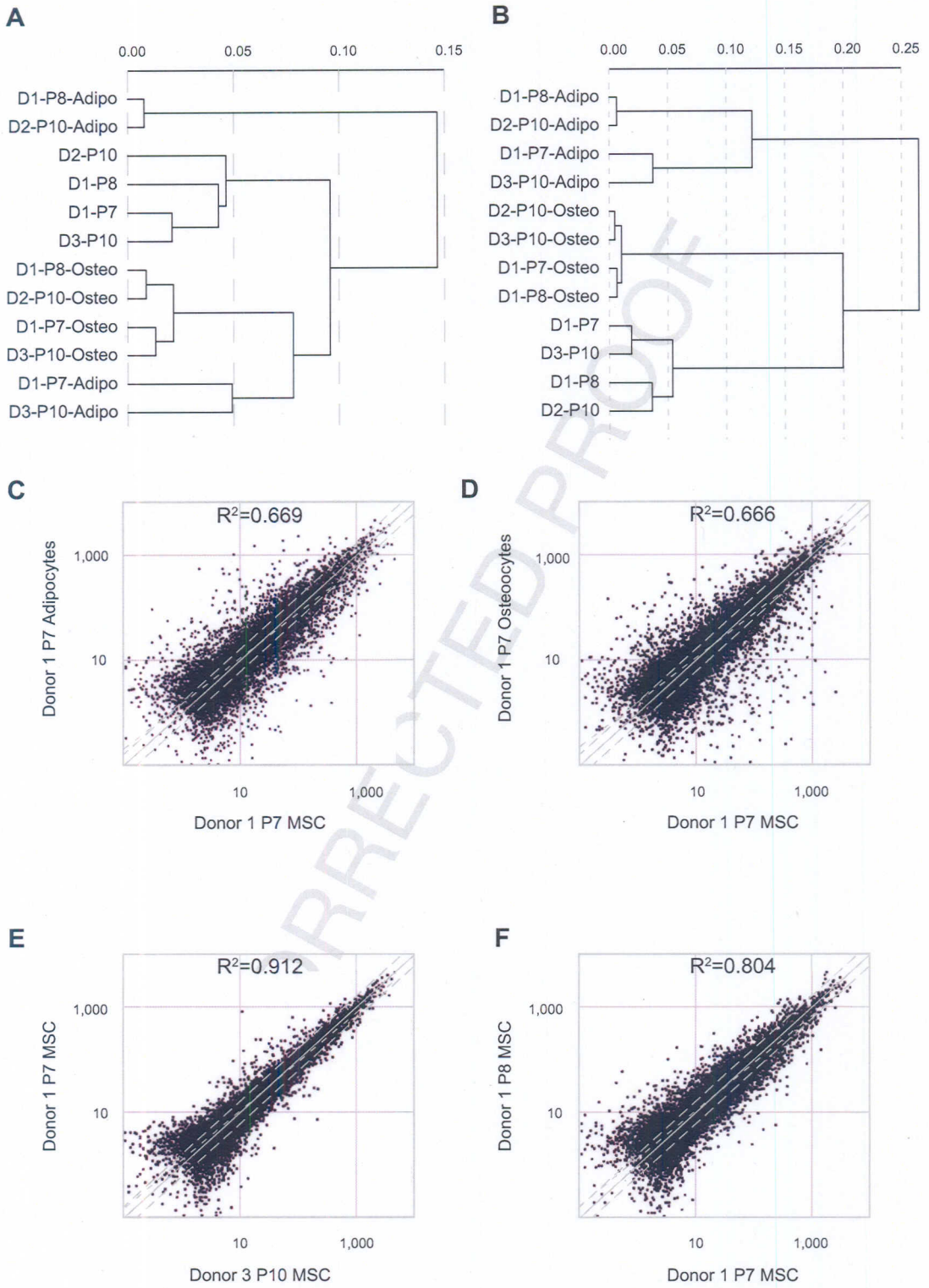

Supplemental Figure 1. Global gene expression analysis of mesenchymal stem cells (MSC) and differentiated adipocytes and osteoblasts. (**A**) Dendrogram plotted with the raw Illumina gene expression date to determine the relatedness of samples. Clustering used Pearson correlation coefficients to calculate the distance metric (1(r). Samples clustered together show greater similarity than samples that are far from each other. (**B**) Dendrogram replotted using analysis ov variance(selected (5% false discovery rate) genes only. The difference between these two dendrograms is largely reflected by the presence in the raw dataset of 24,308 probes having no detectable signal (confidence less than 0.95 in all samples). Scatter plot showing pairwise comparison of global expression detected on Illumina bead array of MSC differentiated into adipocyte (**B**) or osteoblast (**C**). Pattern of expression between MSC from two independent donor bone marrow samples (**D**) and MSC from the same donor differing by 1 passage (**E**) is also shown.